PLoS one

A Possible CO₂ Conducting and Concentrating Mechanism in Plant Stomata SLAC1 Channel

Qi-Shi Du[1,2,4]*, Xina-Wei Fan[2], Cheng-Hua Wang[1,3], Ri-Bo Huang[1,2,3]

1 National Engineering Research Center for Non-Food Biorefinery, Guangxi Academy of Sciences, Nanning, China, 2 College of Life Science and Technology, Guangxi University, Nanning, China, 3 Biotechnology and Pharmaceutical Engineering, Nanjing University of Technology, Nanjing, China, 4 Gordon Life Science Institute, San Diego, California, United States of America

Abstract

Background: The plant SLAC1 is a slow anion channel in the membrane of stomatal guard cells, which controls the turgor pressure in the aperture-defining guard cells, thereby regulating the exchange of water vapour and photosynthetic gases in response to environmental signals such as drought, high levels of carbon dioxide, and bacterial invasion. Recent study demonstrated that bicarbonate is a small-molecule activator of SLAC1. Higher CO_2 and HCO_3^- concentration activates S-type anion channel currents in wild-type Arabidopsis guard cells. Based on the SLAC1 structure a theoretical model is derived to illustrate the activation of bicarbonate to SLAC1 channel. Meanwhile a possible CO_2 conducting and concentrating mechanism of the SLAC1 is proposed.

Methodology: The homology structure of *Arabidopsis thaliana* SLAC1 (AtSLAC1) provides the structural basis for study of the conducting and concentrating mechanism of carbon dioxide in SLAC1 channels. The pK_a values of ionizable amino acid side chains in AtSLAC1 are calculated using software PROPKA3.0, and the concentration of CO_2 and anion HCO_3^- are computed based on the chemical equilibrium theory.

Conclusions: The AtSLAC1 is modeled as a five-region channel with different pH values. The top and bottom layers of channel are the alkaline residue-dominated regions, and in the middle of channel there is the acidic region surrounding acidic residues His332. The CO_2 concentration is enhanced around 10^4 times by the pH difference between these regions, and CO_2 is stored in the hydrophobic region, which is a CO_2 pool. The pH driven CO_2 conduction from outside to inside balances the back electromotive force and maintain the influx of anions (e.g. Cl^- and NO_3^-) from inside to outside. SLAC1 may be a pathway providing CO_2 for photosynthesis in the guard cells.

Introduction

In biology, a stoma is a tiny pore, found in the epidermal tissues of leaves and stems, which is used for gas exchange. The pore is bordered by a pair of kidney-shaped parenchyma cells known as guard cells, which are responsible for regulating the pore aperture of the opening [1]. Ambient carbon dioxide enters the plant leaves through these stomatal pores, where it is used in photosynthesis. Oxygen produced by photosynthesis in the spongy layer cells (parenchyma cells with pectin) of the leaf interior exits through these same openings. In plant respiration the oxygen enters the plant through the stomata, too. Also, water vapor is released into the atmosphere through these pores in a process called transpiration [2,3].

The plant SLAC1 is a slow anion channel in the membrane of stomatal guard cell, which controls the turgor pressure in the aperture-defining guard cells of plant stomata [4–8], thereby regulating the exchange of water vapour and photosynthetic gases in response to environmental signals such as drought, high levels of

carbon dioxide, and bacterial invasion [5,6]. Studies proved that SLAC1 is activated by phosphorylation from the OST1 kinase [9,10]. OST1 activity is negatively regulated by the ABI1 phosphatase [11], which is in turn inhibited by the stomatal ABA receptors PYR and RCAR [12] when in the ternary hormone–receptor–phosphatase complex [13,14]. Thereby, ABA stimulates SLAC1 channel activity. Resulting Cl^- efflux through SLAC1 causes membrane depolarization, which activates outward rectifying K^+ channels, leading to KCl and water efflux to reduce turgor further and cause stomatal closure.

Recent study demonstrated that bicarbonate is a small-molecule activator of SLAC1 [15–17]. Elevated intercellular concentration of HCO_3^- with low concentration of CO_2 and H^+ activated S-type anion channel, whereas low $[HCO_3^-]$ at higher $[CO_2]$ and $[H^+]$ did not [15]. Thereby the bicarbonate activates the SLAC1 anion channels. However, the molecular mechanisms that underlie the SLAC1 activation and stomatal CO_2 signalling have remained relatively obscure. Some logical questions arise from these new findings. How does the concentration of HCO_3^- and CO_2 activate

the SLAC1 to maintain the influx of anions and adjust the pressure in guard cells of stomata? Is there any connection between influx of anions (Cl^- and NO_3^-) and the concentration of HCO_3^- and CO_2 in SLAC1 channel?

Recently an atomic-resolution crystal structure of the TehA from *Haemophilus influenzae* at 1.20 Å resolution was solved by Chen *et al.* [18,19] with the PDB codes 3M71, 3M72, 3M73 and 3M7L (http://www.rcsb.org/pdb/), notably HiTehA (*Haemophilius influenzae* TehA) [19]. Then a homology model of *Arabidopsis thaliana* SLAC1 (AtSLAC1) was developed by Chen *et al.* [18], which is substantially similar to the bacterial homologues. This milestone work provided the structural basis for solving the questions. In this study we perform a theoretical analysis for the activation mechanism of bicarbonate based on the protein structure of AtSLAC1 [18] using physicochemical calculation tools.

Results

The crystal structure of the HiTehA is a trimer consisting of three tightly associated subunits. Each protomer of HiTehA and AtSLAC1 has ten transmembrane helices. The fold of SLAC1 protomer is novel: tandemly repeated helical hairpins are arranged in two layers with quasi-five-fold symmetry. Fig. 1 shows the alignment of AtSLAC1 model structure and its template HiTehA. The backbones of two structures overlap very nicely. The extracellular inter-helix loops are short (1–5 residues), whereas the intracellular inter-helix connections are longer (Fig. 1 A). The top (outside the membrane) and the bottom (inside the membrane) of the SLAC1 channel are filled by water molecules. In Fig. 1 the residue Phe262 (colored in yellow) is in the center of stomatal channel, which is the gate of the channel. The ten helices of the two layers in SLAC1 channel are connected by flexible loops. It is anticipated that the 'triple-barrel' structure of the AtSLAC1 channel makes the diameter of the channel is adjusted by pressure change in the guard cells.

The subcellular location of SLAC1 was experimentally determined in the surface of the guard cell using combined SLAC1 protein and green fluorescent protein. Further experiment examined that the SLAC1 is in the plasma membrane [20]. Therefore, the SLAC1 is a plasma-membrane-localized protein in the guard cells, and participates in the control of anion fluxes across the plasma membrane of guard cells [18,20].

Amino acid composition of AtSLAC1

The amino acid composition and distribution in HiTehA and AtSLAC1 are shown in Fig. 2, where the acidic residues are colored in pink, alkaline residues in blue, polar residues in light blue, and hydrophobic residues in light green. The channel gate 262Phe (in HiTehA) and 462Phe (in AtSLAC1) are shown in yellow. The acidic and alkaline residues are shown in space filling render. Most alkaline residues (blue) and acidic residues (pink) concentrate locate in the top layer and bottom layer of the channel. The hydrophobic residues (light green) are in the middle, the transmembrane part of the channel.

The values of acidic ionizing constant (pK_a) of residues are essential for the CO_2 conducting and concentrating. The classification of 20 natural amino acids is listed in Table 1. In Table 1 the pK_a values of amino acid side chains are only the model values [21]. The effective pK_a values of residues in the protein may be very different from the model values because of the special protein environment. The pK_a values of ionizable residues in AtSLAC1 are calculated using software PROPKA3.0 [21–23] and listed in Table 2.

In Table 2 there are 44 alkaline residues and 16 acidic residues. Most acidic and alkaline residues are located in the top and the bottom of AtSLAC1 channel. The amino acid distribution in the top layer of AtSLAC1 channel is shown in **Fig. 3 A** and **B**. In the top
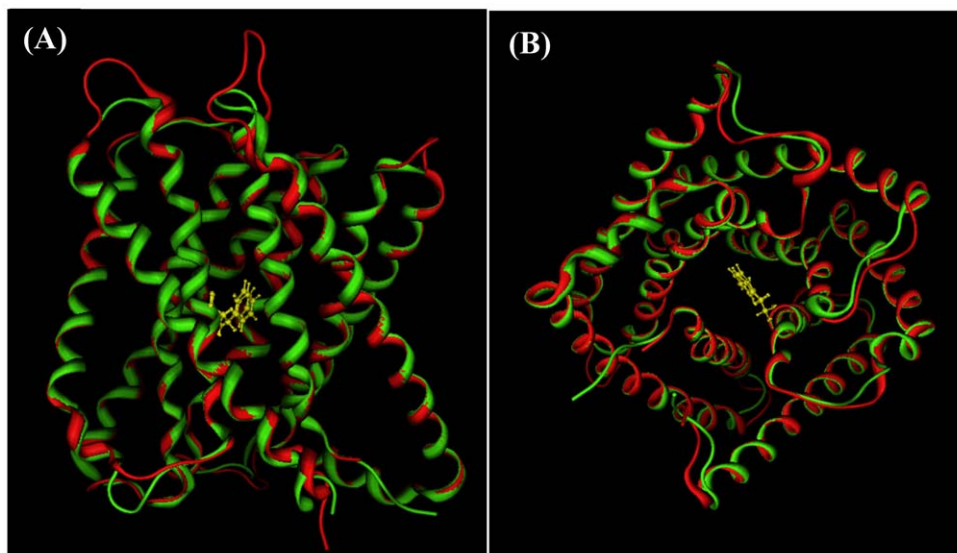

Figure 1. The structural alignment of *Arabidopsis thaliana* SLAC1 (AtSLAC1) homology structure and the template structure *Haemophilius influenzae* TehA (HiTehA). The backbone of AtSLAC1 is shown in red and the HiTehA is in green. (**A**) A side view of AtSLAC1 and HiTehA alignment. The backbones of two structures overlap very nicely. (**B**) A top view of AtSLAC1 and HiTehA alignment. The ten helical hairpins are arranged in two layers with quasi-five-fold symmetry. The residue Phe262 (colored in yellow) is in the center of channel, which is the gate of the channel. The ten helices of the two layers in SLAC1 channel are connected by flexible loops. It is anticipated that the diameter of the SLAC1 channel can be adjusted by pressure change in the guard cell.
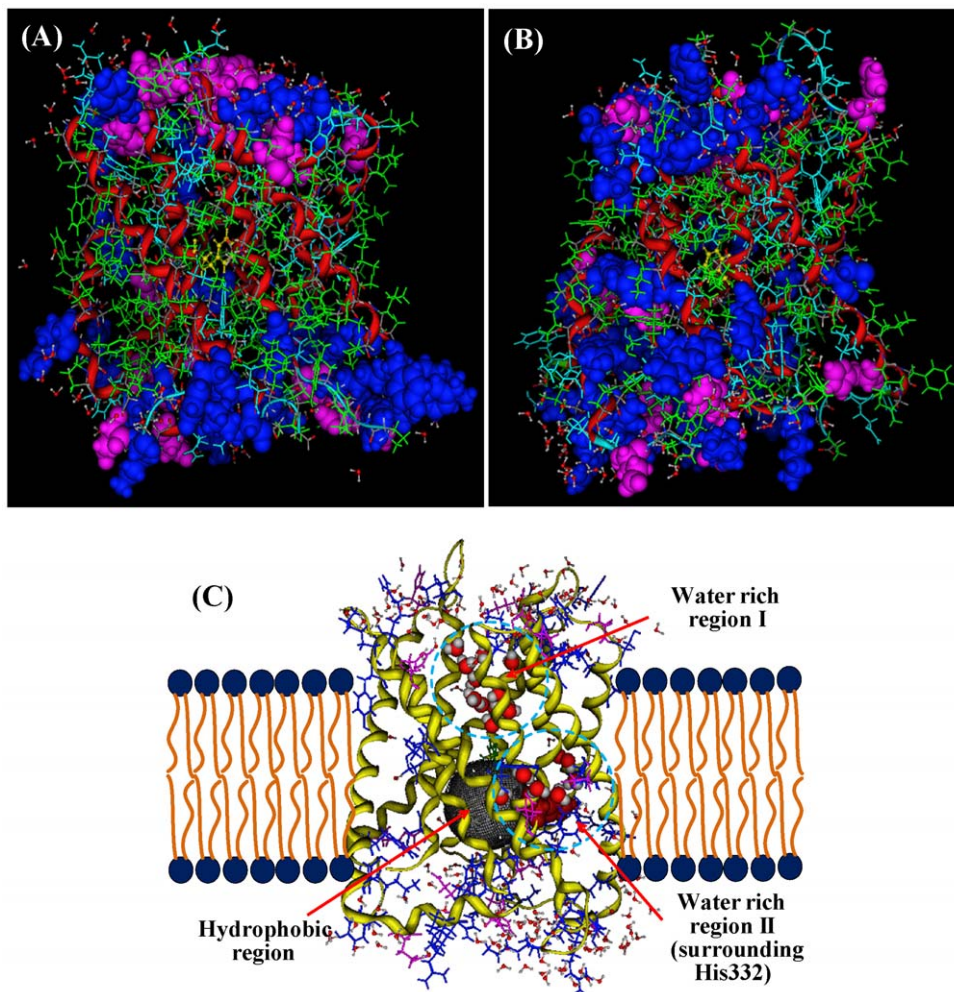doi:10.1371/journal.pone.0024264.g001

Figure 2. Amino acid distributions in *Arabidopsis thaliana* SLAC1 (AtSLAC1) and in *Haemophilius influenzae* TehA (HiTehA). (**A**) Amino acid distributions of AtSLAC1. The acidic residues are shown in blue space filling render, and the acidic residues in pink space filling render. The polar residues are in light blue line drawing, and the hydrophobic residues are in light green line drawing. (**B**) Amino acid distributions of HiTehA. The acidic residues (pink) and the alkaline residues (blue) are concentrated in top and bottom layers, and the hydrophobic residues (light green) are arranged in the middle of the channel. (**C**) The transmembrane model of AtSLAC1. The top and bottom layers are filled by water molecules. In the channel there are two water-rich regions, in which the water molecules are shown in space filling drawing. The dark gray ball indicates the hydrophobic region, where is an empty cavity.
doi:10.1371/journal.pone.0024264.g002

layer there are five acidic residues (His219, His293, Asp351, Asp412, and Glu464) and 14 alkaline residues (Lys211, Arg289, Lys290, Tyr291, Lys347, Lys355, Tyr408, Cys414, Arg416, Cys418, Lys61, Tyr462, Tyr469, and Arg472). In the bottom layer, as shown in **Fig. 3 C** and **D**, there are 7 acidic residues (Glu252, Glu257, His260, Glu380, Glu385, His387, and His496) and 20 alkaline residues (Cys192, Tyr243, Lys246, Cys247, Tyr250, Lys255, Arg256, Tyr258, Arg263, Lys310, Lys320, Arg321, Arg322, Cys324, Lys325, Tyr373, Arg375, Lys384, Tyr390, and Lys440). In both top layer and bottom layer the alkaline residues exceed the acidic residues much more. The alkaline condition in the top and bottom layers is in favor of CO$_2$ absorption and storage.

CO$_2$ conducting mechanism

Fig. 4 shows the cartoon model of the AtSLAC1 stomatal channel, which is used to illustrated the conducting mechanism of carbon dioxide. The SLAC1 channel is divided into five regions. The first region is the top layer of SLAC1 channel, which is modeled as an alkaline aqueous solution, because it is dominated

by alkaline residues and filled by water molecules. Below the first region there is a water pool, the second region in the channel, which is surrounded by polar residues and filled by water molecules. In Fig. 4 the third region is also filled by water molecules, surrounding the acidic residue His332 (space filling render in dark red), which has the second lowest pK$_a$ value (pK$_a$ = 3.65) in Table 2. The fourth region is a hydrophobic region, formed mainly by hydrophobic residues, which is an empty cavity. The fifth region is the bottom layer of the channel, which is formed by alkaline and acidic residues and filled by water molecules. The fifth region is an alkaline solution, because where are much more alkaline residues (blue) than the acidic residues (pink). However, in the bottom layer there are one or two acidic exits of CO$_2$ formed by the acidic residues.

The carbon dioxide conducting mechanism can be illustrated based on the cartoon model of SLAC1 channel in Fig. 4. The CO$_2$ conductance is a six-step procedure. The CO$_2$ is first absorbed from the atmosphere into the alkaline solution in the region 1, forming hydrogen carbonate ion HCO$_3^-$. In the second step the HCO$_3^-$

Table 1. Chemical properties and classification of 20 natural amino acids.

Amino acid	pK$_a$*	Classification
Asp (D)	3.93	Acidic
Glu (E)	4.37	Acidic
His (H)	6.50	Acidic
Arg (R)	12.50	Alkaline
Lys (K)	10.50	Alkaline
Tyr (Y)	10.00	Alkaline
Cys (C)	9.00	Alkaline
Ser (S)	-	Polar
Thr (T)	-	Polar
Asn (N)	-	Polar
Gln (Q)	-	Polar
Trp (W)	-	Polar
Gly (G)	-	Hydrophobic
Ala (A)	-	Hydrophobic
Val (V)	-	Hydrophobic
Leu (L)	-	Hydrophobic
Ile (I)	-	Hydrophobic
Met (M)	-	Hydrophobic
Phe (F)	-	Hydrophobic
Pro (P)	-	Hydrophobic

*The referent pK$_a$ values are from references [18–20].

doi:10.1371/journal.pone.0024264.t001

Table 2. The pKa values of ionizable residues in AtSLAC1.

Acidic Residues			Alkaline Residues		
No.	A.A.	pK$_a$	No.	A.A.	pK$_a$
351	ASP	3.93	192	CYS	10.68
412	ASP	2.41	196	CYS	12.10
252	GLU	4.37	247	CYS	9.78
257	GLU	5.79	274	CYS	11.49
308	GLU	4.48	298	CYS	9.47
352	GLU	4.66	324	CYS	8.64
380	GLU	4.58	414	CYS	9.61
385	GLU	4.35	418	CYS	10.18
464	GLU	7.03	487	CYS	9.37
219	HIS	6.73	243	TYR	13.83
260	HIS	4.28	250	TYR	10.12
293	HIS	6.02	258	TYR	11.73
332	HIS	3.65	291	TYR	10.79
364	HIS	5.67	304	TYR	11.06
387	HIS	4.52	312	TYR	10.31
496	HIS	5.98	365	TYR	13.99
			373	TYR	10.23
			390	TYR	12.32
			408	TYR	10.38
			426	TYR	10.56
			448	TYR	11.41
			462	TYR	13.40
			469	TYR	10.04
			211	LYS	10.07
			246	LYS	9.86
			255	LYS	10.56
			290	LYS	10.03
			310	LYS	9.20
			320	LYS	9.64
			325	LYS	10.10
			347	LYS	10.05
			355	LYS	9.73
			384	LYS	9.93
			440	LYS	10.44
			461	LYS	9.12
			256	ARG	12.55
			263	ARG	12.14
			289	ARG	12.36
			321	ARG	12.15
			322	ARG	12.57
			375	ARG	11.25
			416	ARG	9.90
			432	ARG	12.41
			472	ARG	12.39

doi:10.1371/journal.pone.0024264.t002

migrates to the aqueous solution in the region 2. Then in the third step the ion HCO_3^- enters the acidic region 3 centered by His332 (pK$_a$ = 3.65), where it dissociates to CO_2 in the acidic condition. In the fourth step the saturated CO_2 in the acidic region 3 comes to the hydrophobic region 4, which is a carbon dioxide storage pool. In the fifth step, from the carbon dioxide pool the CO_2 dissolves in the alkaline solution in the region 5, forming hydrogen carbonate ion HCO_3^-. Finally in the sixth step, the ion HCO_3^- dissociates to CO_2 in the acidic exit of the region 5, and comes to the cell plasma through the acidic exit. The step 1, transfer of CO_2 from atmosphere to region 1, is a gas-solution equilibrium process. The step 2 of HCO_3^- migration from region 1 to region 2 is caused by concentration gradient. The steps 4 and 5 are also the gas-solution equilibrium process. The reversible conversion of CO_2 to HCO_3^- is driven by pH differences between different regions. It is much faster than the conversion in uniform solution with constant pH value.

CO₂ concentrating mechanism

The CO_2 conductance from atmosphere to cell plasma through SLAC1 channel enhances the CO_2 concentration remarkably. Assuming in atmosphere the concentration of carbon dioxide is $[CO_2]_{air}$ and the pH value in alkaline solution of the region 1 is pH = 9.0, the concentration of hydrogen carbonate ion HCO_3^- is calculated as follows.

$$CO_2(g) + H_2O(l) \_ HCO_3^-(aq) + H^+(aq), K_a = 4.60 \_ 10^{-7} \text{ mol/L}$$

$$\frac{[HCO_3^-][H^+]}{[CO_2]_{air}} = K_a$$

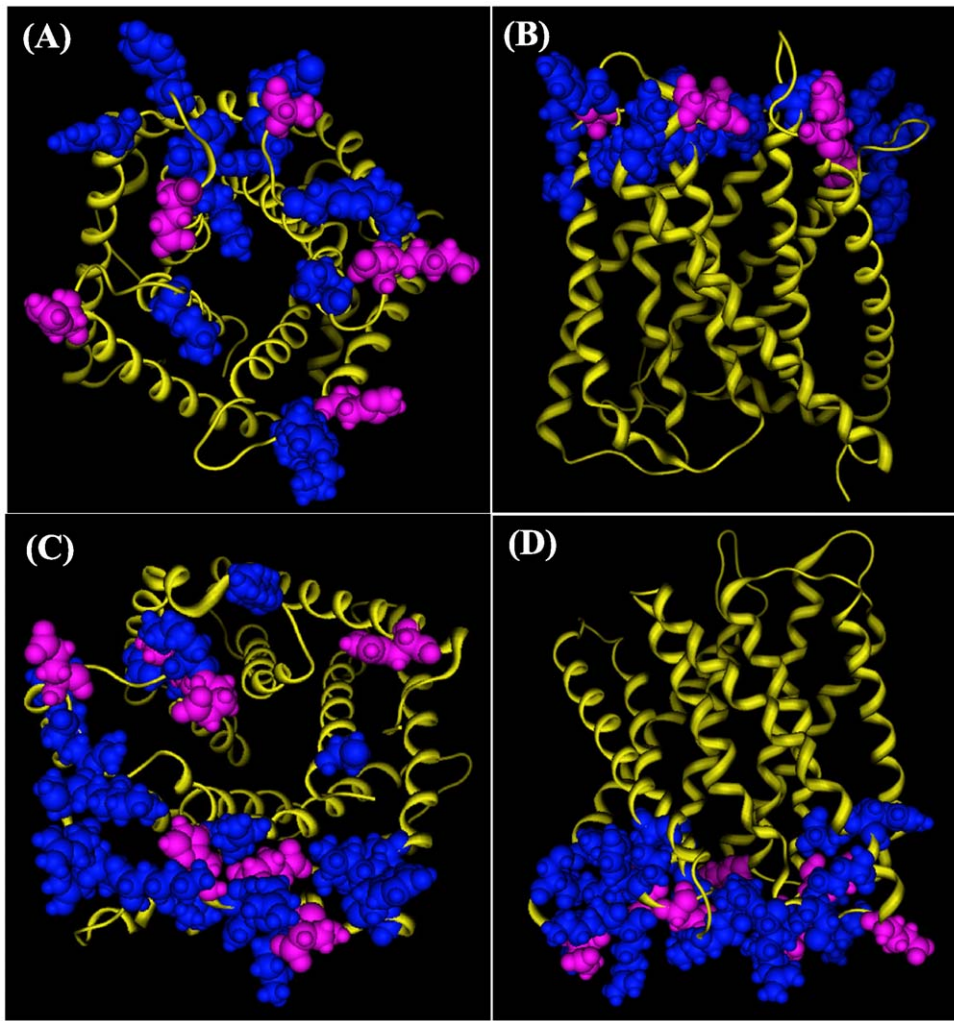$$[HCO_3^-] = \frac{[CO_2]_{air}}{[H^+]} K_a = 10^9 [CO_2]_{air} K_a$$

Figure 3. Acidic residues (pink) and alkaline residues (blue) in the top and bottom layers of AtSLAC1 channel. (A) A top view of the residue distribution in the top layer. **(B)** A side view of the residue distribution in the top layer. In the top layer there are five acidic residues (His219, His293, Asp351, Asp412, and Glu464) and 14 alkaline residues (Lys211, Arg289, Lys290, Tyr291, Lys347, Lys355, Tyr408, Cys414, Arg416, Cys418, Lys61, Tyr462, Tyr469, and Arg472). **(C)** A bottom view of the residue distribution in the bottom layer. **(D)** A side view of the residue distribution in the bottom layer. In the bottom layer there are 7 acidic residues (Glu252, Glu257, His260, Glu380, Glu385, His387, and His496) and 20 alkaline residues (Cys192, Tyr243, Lys246, Cys247, Tyr250, Lys255, Arg256, Tyr258, Arg263, Lys310, Lys320, Arg321, Arg322, Cys324, Lys325, Tyr373, Arg375, Lys384, Tyr390, and Lys440). Both top and bottom layers are alkaline residue-dominated region, and filled by water molecules.
doi:10.1371/journal.pone.0024264.g003

In the acidic region 3 surrounding His332, the hydrogen carbonate ion HCO_3^- dissociates to CO_2. This is just the reverse reaction of the above equation, $K_b = K_a^{-1}$. Assuming in the acidic region 3 the pH value is 5.0, the concentration $[CO_2]_3$ in region 3 is calculated as follows.

$$HCO3\_(aq) + H + (aq)\_CO2(g) + H2O(1), \quad Kb = Ka - 1$$
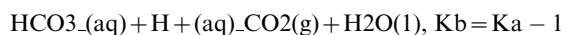
$$\frac{[CO_2]_3}{[HCO_3^-][H^+]} = K_b$$

$$\frac{[CO_2]_3}{[HCO_3^-][H^+]} = K_b$$

$$[CO_2]_3 = [HCO_3^-][H^+]K_b = 10^4[CO_2]_{air}$$

Therefore, the CO_2 concentration in the region 3 of SLAC1 channel is 10^4 times higher than the concentration in the atmosphere.

The above calculation for CO_2 concentrating mechanism is not rigorous because of the following two problems. The first problem is that the calculation uses the assumed pH values in the alkaline solutions (pH = 9) and in the acidic regions (pH = 5). The second problem is that the chemical equilibrium equation holds for macro system, however, the SLAC1 channel is not a macro system. Although the above calculation is not rigorous, it still can be used to illustrate the CO_2 concentrating in the SLAC1 channel qualitatively. If the alkaline residues and acidic residues in the first, third, and fifth regions are treated as the donors and receptors of H^+, OH^-, and HCO_3^-, we can get the same qualitative results.
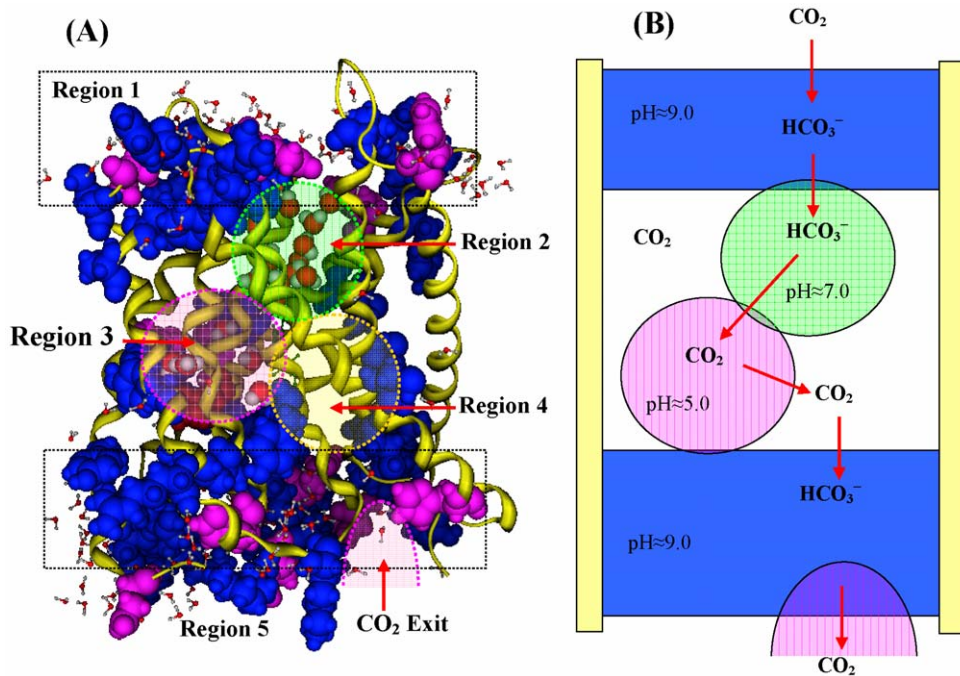
Figure 4. The cartoon model of the AtSLAC1 channel for illustrating CO2 conducting mechanism and concentrating mechanism. (A) Five regions of AtSLAC1 channel. The top layer and bottom layer are the region 1 and region 5, respectively. Inside the channel the water-rich region below the top layer is the region 2, and another water rich-region surrounding acidic residue His332 is region 3. The hydrophobic region is the region 4. **(B)** The cartoon model of plant AtSLAC1 channel. The region 1 and region 5 (top and bottom layer) are modeled as alkaline solution (pH≈9.0). The region 2 is neural aqueous solution (pH≈7.0), and region 3 is an acidic region (pH≈5.0), because the residue His332 possesses the very lower pKa value (pKa = 3.65). The hydrophobic region 4 is a CO_2 storage pool.
doi:10.1371/journal.pone.0024264.g004

If the concentration (partial pressure) of CO_2 in atmosphere is $[CO_2]_{air} = 0.0003$ atm, according to the above calculations, the CO_2 concentration in the hydrophobic region 4 (CO_2 pool) is

$$[CO_2]_{pool} = 10^4[CO_2]_{air} = 3.0 \text{ atm}$$

The very high concentration of CO_2 in AtSLAC1 channel may be over estimated. However, the carbon dioxide concentration in plant SLAC1 channel must be higher than that in the atmosphere.

Activation mechanism of SLAC1

Recent study revealed that the bicarbonate is a small-molecule activator of SLAC1 [15]. The activation mechanism of HCO_3^- to AtSLAC1 can be illustrated based on the CO_2 conduction and concentration model of AtSLAC1 proposed in this study. The *Arabidopsis thaliana* SLAC1 was identified as a slow anion channel [18]. Study shows that electrostatic features of the pore coupled with electrophysiological characteristics indicate that selectivity among different anions is largely a function of the energetic cost of ion dehydration [18]. The relative anion permeability sequence of SLAC1 is $I^- > NO_3^- > Br^- > Cl^-$ [18,24,25]. The SLAC1 channel transports anions (Cl^- and NO_3^-) from inside of guard cell to outside cross the membrane. The one-way conduct will make the electrostatic potential inside the guard cell is higher than the outside. The back electromotive force will stop the conduction. On the other hand, the conduction of anion HCO_3^- through SLAC1 channel is from outside to inside of the guard cell driven by pH difference. The difference between anion HCO_3^- and other anions (I^-, NO_3^-, Br^-, and Cl^-) is that the anion HCO_3^- is pH sensitive, which has higher concentration in alkaline solution, and

dissociates to CO_2 in acidic solution. Therefore, pH value has strong modulation ability to anion HCO_3^- than to other anions. The conduction of CO_2 (in HCO_3^- form) in SLAC1 channel from outside to inside is a necessary condition to balance the back electromotive force and maintain the influx of other anions (Cl^-, NO_3^-, I^- and Br^-) from inside to outside. In this way the bicarbonate plays the role of activator for SLAC1 channel.

Discussion

Usually the reversible conversion of between CO_2 and HCO_3^- is a very slow process without the catalysis by carbonic anhydrases. This is the phenomena of the conversion between CO_2 and HCO_3^- in a uniform solution with constant pH value. The proposed model of SLAC1 channel consists of several regions with different pH values. This is only possible in a micro channel. Just the different pH values elevate the concentration of CO_2, and make the conversion between CO_2 and HCO_3^- much faster than in uniform macro solution. This is like the case when a drop of hydrochloric acid is put in $NaHCO_3$ solution, the CO_2 escapes out quickly.

The function of CO_2 conduction and concentration of SLAC1 channel is highly interesting, because it implies a possible pathway of CO_2 supply in plant. As we known the stomatal aperture is the regular pathway of CO_2 supplying to cells in leaves for photosynthetic reactions. However, the pathway of CO_2 influx to the guard cells self is unclear. The proposed mechanism of CO_2 conduction and concentration indicates that the SLAC1 channel may be a possible pathway providing CO_2 for photosynthesis in guard cells. The high concentration of CO_2 (or HCO_3^-) in the plant SLAC1 channel not necessarily means the high concentration of CO_2 (or HCO_3^-) in guard cells, because the transfer of

CO$_2$ (or HCO$_3^-$) in cell plasma of guard cells to the enzyme RuBisCo needs the help of enzyme CA (carbonic anhydrase) [26–31]. However, the CO$_2$ concentrating in SLAC1 channel may be a mechanism dealing with the instant fluctuation of carbon dioxide in environment.

The possible function of CO$_2$ conduction and concentration in SLAC1 channel is supported by the water-channel protein aquaporin [32–35]. The role of aquaporin in CO$_2$ diffusion in higher plants was first examined by Terashima and Ono [36]. A significant decrease of g_i (internal CO$_2$ conductance) was detected in the presence of HgCl$_2$, an inhibitor of most aquaporins, which is the evidence indicating involvement of aquaporins in CO$_2$ diffusion across the plasma membrane [36]. Then the role of aquaporin in CO$_2$ diffusion inside plant leaves was further confirmed by Hanba et al. [37].

In the cartoon model of AtSLAC1 channel (Fig. 4), the top region and bottom region are modeled as the alkaline solutions. However, the two regions are best to be described as the alkaline buffer solutions, because of the alternately distribution of alkaline residues and acidic residues. The alkaline residue-dominated buffer solution not only can maintain the constantly higher pH value, but also can accommodate more CO$_2$ (or HCO$_3^-$). In the AtSLAC1 model the acidic His332 in the region 3 plays an important role, by which the CO$_2$ concentration in the hydrophobic region (CO$_2$ pool) is enhanced greatly. Actually, histidine can play the role of both proton donor and acceptor. The transfer of HCO$_3^-$ to CO$_2$ at the His332 may be the speed-control step in the slow anion channel.

Carbon dioxide is a key reactant in plant photosynthesis. The continuing rise in of green house gas CO$_2$ in atmosphere is predicted to have diverse and dramatic effects on the productivity of agriculture, plant ecosystems, and global climate [38–40]. The CO$_2$ conducting mechanism and concentrating mechanism in plant SLAC1 channel, derived in this study based on the structure of AtSLAC1, may provide useful insight into this important research topic.

Materials and Methods

Amino acid classification and pK$_a$ calculation

The plant SLAC1 anion channel has a novel amino acid composition, and its unique mechanism for CO$_2$ conductance can be illustrated using the physicochemical properties of amino acids. The properties of 20 natural amino acids and the pK$_a$ values of side chains are listed in Table 1. The 20 amino acids are classified into four types: acidic, alkaline, polar, and hydrophobic. In this study the acidic residues includes Asp, Glu and His, and the alkaline residues are Arg, Lys, Tyr, and Cys [21–23]. Five amino acids (Ser, Thr, Asn, Gln, and Trp) are classified as the polar residues. The remaining 8 amino acids are hydrophobic residues. In Table 1 the pK$_a$ values of ionizable amino acid side chains are model values [23], which may be very different from the effective pK$_a$ values in protein environment.

The effective pK$_a$ values of ionizable amino acids in HiTehA and AtSLAC1 are calculated using software PROPKA3.0 [21-23].

$$pK_a(\text{pro}) = pK_a(\text{mod}) + \frac{1}{2.303kT}\Delta G$$

In the above calculation equation the ΔG is the free energy change of a residue side chain from exposed environment to the protein fold environment. When a protein folds, the titratable amino acids in the protein are transferred from a solution-like environment to an environment determined by the 3-D structure of the protein. In the unfolded protein the titratable side chain of amino acid typically exposes to water. When the protein folds the side chain could be buried deeply in the protein interior with no exposure to solvent. Furthermore, in the folded protein the side chain may be closer to other titratable groups in the protein and will also interact with permanent charges (e.g. ions) and dipoles in the protein. All of these effects alter the pK$_a$ value of the amino acid side chain. The pK$_a$ calculation methods generally calculate the effect of the protein environment on the model pK$_a$ value of an amino acid side chain.

Calculation of pH value in CO$_2$ solution

The CO$_2$ conducting and concentrating mechanism of plant SLAC1 channel relate with the unique physicochemical properties of carbon dioxide. When carbon dioxide dissolves in water, it exists in equilibrium with carbonic acid.

$$CO2 + H2O \_ H2CO3$$
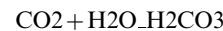
Carbonic acid is diprotic having two protons, which may dissociate from the parent molecule. Thus there are two dissociation constants.

$$H2CO3 \_ HCO3 \_ + H+, \ Ka1 = 4.45 \_ 10 \_ 7$$
$$HCO3 \_ CO32 \_ + H+, \ Ka2 = 4.69 \_ 10 \_ 11$$
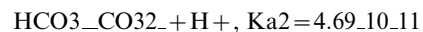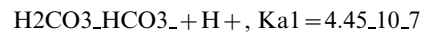
The first one is the dissociation into the hydrogen carbonate ion HCO$_3^-$, and the second is the dissociation of the bicarbonate ion into the carbonate ion CO$_3^{2-}$. However, in aqueous solution carbonic acid only exists in equilibrium with carbon dioxide, and the concentration of H$_2$CO$_3$ is much lower than the dissolved CO$_2$ concentration. Since it is not possible to distinguish between H$_2$CO$_3$ and dissolved CO$_2$ by conventional methods, the dissolving and ionizing equation of CO$_2$ in aqueous solution may be rewritten as follows,

$$CO2 + H2O \_ HCO3 \_ + H+, \ Ka = 4.60 \_ 10\text{-}7 \ mol/L$$
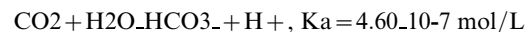
Whereas this K$_a$ is quoted as the dissociation constant of carbonic acid, and it might better be referred to as the acidity constant of dissolved carbon dioxide, as it is particularly useful for calculating the pH of CO$_2$-containing solutions. In the alkaline solution, the higher pH value (lower concentration [H$^+$]) is favor in CO$_2$ dissolution (higher concentration [HCO$_3^-$]). On the other hand, lower pH value (higher concentration [H$^+$]) makes the HCO$_3^-$ to dissociate to CO$_2$.

Author Contributions

Conceived and designed the experiments: QSD RBH. Performed the experiments: QSD CHW. Analyzed the data: QSD CHW. Contributed reagents/materials/analysis tools: QSD XWF. Wrote the paper: QSD RBH.

References

1. Esau K (1977) Anatomy of Seed Plants. Wiley and Sons. 88 p.
2. Nadeau JA, Sack FD (2002) Control of stomatal distribution on the Arabidopsis leaf surface. Science 296: 1697–1700.
3. Sirichandra C, Wasilewska A, Vlad F, Valon C, Leung J (2009) The guard cell as a single-cell model towards understanding drought tolerance and abscisic acid action. J Exp Bot 60: 1439–1463.
4. Liu J, Elmore JM, Fuglsang AT, Palmgren MG, Staskawicz BJ, et al. (2009) RIN4 functions with plasma membrane H⁺-ATPases to regulate stomatal apertures during pathogen attack. PLoS Biology 7: e1000139.
5. Nurnberger T, Kemmerling B (2006) Receptor protein kinases– pattern recognition receptors in plant immunity. Trends Plant Sci 11: 519–522.
6. Melotto M, Underwood W, Koczan J, Nomura K, He SY (2006) Plant stomata function in innate immunity against bacterial invasion. Cell 126: 969–980.
7. Lee SC, Lan W, Buchanan BB, Luan S (2009) A protein kinase-phosphatase pair interacts with an ion channel to regulate ABA signaling in plant guard cells. Proc Natl Acad Sci USA 106: 21419–21424.
8. Geiger D, Scherzer S, Mumm P, Stange A, Marten I, et al. (2009) Activity of guard cell anion channel SLAC1 is controlled by drought-stress signaling kinase-phosphatase pair. Proc Natl Acad Sci USA 106: 21425–21430.
9. Schroeder JL, Hagiwara S (1989) Cytosolic calcium regulates ion channels in the plasma membrane of vicia faba guard cells. Nature 338: 427–430.
10. Mustilli A, Merlot S, Vavasseur A, Fenzi F, Giraudat J (2002) Arabidopsis OST1 protein kinase mediates the regulation of stomatal aperture by abscisic acid and acts upstreamof reactive oxygen species production. Plant Cell 14: 3089–3099.
11. Meyer K, Leube MP, Grill E (1994) A protein phosphatase 2C involved in ABA signal transduction in Arabidopsis thaliana. Science 264: 1452–1455.
12. Ma Y, Szostkiewicz I, Korte A, Moes D, Yang Y, et al. (2009) Regulators of PP2C phosphatase activity function as abscisic acid sensors. Science 324: 1064–1068.
13. Melcher K, Ng L-M, Zhou XD, Soon F-F, Xu Y, et al. (2009) A gate-latch-lock mechanism for hormone signalling by abscisic acid receptors. Nature 462: 602–608.
14. Fujii H, Chinnusamy V, Rodrigues A, Rubio S, Antoni R, et al. (2009) In vitro reconstitution of an abscisic acid signalling pathway. Nature 462: 660–664.
15. Xue S, Hu H, Ries A, Merilo E, Kollist H, et al. (2011) Central functions of bicarbonate in S-type anion channel activation and OST1 protein kinase in CO₂ signal transduction in guard cell. EMBO J 30: 1645–1658.
16. Hu H, Boisson-Dernier A, Israelsson-Nordstrom M, Bohmer M, Xue S, et al. (2010) Carbonic anhydrases are upstream regulators of CO₂-controlled stomatal movements in guard cells. Nat cell Biol 12: 87–93.
17. Hashimoto M, Negi J, Young J, Israelsson M, Schroeder JI, et al. (2006) Arabidopsis HT1 kinase controls stomatal movements in response to CO2. Nature Cell Biol 8: 391–397.
18. Chen Y, Hu L, Punta M, Bruni R, Hillerich B, et al. (2010) Homologue structure of the SLAC1 anion channel for closing stomata in leaves. Nature 467: 1074–1080.
19. Taylor DE, Hou Y, Turner RJ, Weiner JH (1994) Location of a potassium tellurite resistance operon (tehA tehB) within the terminus of Escherichia coli K-12. J Bacteriol 176: 2740–2742.
20. Negi J, Matsuda O, Nagasawa T, Oba Y, Takahashi H, et al. (2008) CO₂ regulator SLAC1 and its homologues are essential for anion homeostatsis in plant cells. Nature 452: 483–486.
21. Olsson MHM, Søndergaard CR, Rostkowski M, Jensen JH (2011) PROPKA3: consistent treatment of internal and surface residues in empirical pKa predictions. J Chem Theory Comput 7: 525–537.
22. Bas DC, Rogers DM, Jensen JH (2008) Very fast prediction and rationalization of pKa values for protein-ligand complexes. PROTEINS: Structure, Function, and Bioinformatics 73: 765–783.
23. Li H, Robertson AD, Jensen JH (2005) Very fast empirical prediction and rationalization of protein pKa values. PROTEINS: Structure, Function, and Bioinformatics 61: 704–721.
24. Dutzler R, Campbell EB, MacKinnon R (2003) Gating the selectivity filter in ClC chloride channels. Science 300: 108–112.
25. Picollo A, Malvezzi M, Houtman JC, Accardi A (2009) Basis of substrate binding and conservation of selectivity in the CLC family of channels and transporters. Nature Struct. Mol Biol 16: 1294–1301.
26. Colcombet J, Lelièvre F, Thomine S, Barbier-Brygoo H, Frachisse JM (2005) Distinct pH regulation of slow and rapid anion channels at the plasma membrane of Arabidopsis thaliana hypocotyl cells. J Expt Botany 56: 1897–1903.
27. Badger MR, Price GD (1994) The role of carbonic anhydrase in photosynthesis. Annu Rev Plant Physiol Plant Mol Biol 45: 369–392.
28. Raven JA (1997) CO₂-concentrating mechanisms: a direct role for thylakoid lumen acidification. Plant Cell Environ 20: 147–154.
29. Kaplan A, Reinhold L (1999) CO₂ concentrating mechanisms in photosynthetic microorganisms. Annu Rev Plant Physiol Plant Mol Biol 50: 539–570.
30. Moroney JV, Somanchi A (1999) How do algae concentrate CO₂ to increase the efficiency of photosynthetic carbon fixation? Plant Physiol 119: 9–16.
31. Badger MR, Spalding MH (2000) CO₂ acquisition, concentration and fixation in cyanobacteria and algae. In S von Caemmerer, ed, Photosynthesis: Physiology and Metabolism. Kluwer Academic Publishers, Dordrecht, The Netherlands. pp 369–397.
32. Agre P (2006) The aquaporin water channels. Proc Am Thorac Soc 3: 5–13.
33. Agre P, Kozono D (2003) Aquaporin water channels: molecular mechanisms for human diseases. FEBS Lett 555: 72–78.
34. Schrier RW (2007) Aquaporin-related disorders of water homeostasis. Drug News Perspect 20: 447–53.
35. Knepper MA, Nielsen S (2004) Peter Agre, 2003 Nobel Prize winner in chemistry. J Am Soc Nephrol 15: 1093–5.
36. Terashima I, Ono K (2002) Effects of HgCl₂ on CO₂ dependence of leaf photosynthesis: evidence indicating involvement of aquaporins in CO₂ diffusion across the plasma membrane. Plant Cell Physiol 43: 70–78.
37. Hanba YT, Shibasaka M, Hayashi Y, Hayakawa T, Kasamo K, et al. (2004) Overexpression of the barley aquaporin HvPIP2;1 increases internal CO₂ conductance and CO₂ assimilation in the leaves of transgenic rice plants. Plant Cell Physiol 45: 521–529.
38. Hetherington AM, Woodward FI (2003) The role of stomata in sensing and driving environmental change. Nature 424: 901–908.
39. Sellers PJ, Dickinson RE, Randall DA, Betts AK, Hall FG, et al. (1997) Modeling the exchanges of energy, water, and carbon between continents and the atmosphere. Science 275: 502–509.
40. Shaw MR, Zavaleta ES, Chiariello NR, Cleland EE, Mooney HA, et al. (2002) Grassland responses to global environmental changes suppressed by elevated CO2. Science 298: 1987–1990.